BULLETIN OF THE POLISH ACADEMY OF SCIENCES
TECHNICAL SCIENCES,
DOI: 110.24425/bpasts.2024.152608

Towards backward compatibility of ADRC: revisiting classical state-feedback control with integral compensator

Mikołaj Mrotek[1] **Jacek Michalski**[1]* **Rafal Madonski**[2] **Dariusz Pazderski**[3] **Marek Retinger**[1]

[1] Faculty of Control, Robotics and Electrical Engineering, Institute of Robotics and Machine Intelligence, Poznan University of Technology, Piotrowo 3a, 60-965 Poznan, Poland

[2] Faculty of Automatic Control, Electronics and Computer Science, Department of Automatic Control and Robotics, Silesian University of Technology, Akademicka 16, 44-100, Gliwice, Poland

[3] Faculty of Control, Robotics and Electrical Engineering, Institute of Automatic Control and Robotics, Poznan University of Technology, Piotrowo 3a, 60-965 Poznan, Poland

Abstract. In this paper, the problem of backward compatibility of active disturbance rejection control (ADRC) is investigated. The goal is to contextualize ADRC to deliver its interpretations from the established field of linear control systems. For this study, a control algorithm, denoted here as integral disturbance rejection control (IDRC), is considered that combines classical state-feedback control with an integral compensator. At first, an interpretation of ADRC is involved in terms of existing state-space control approaches. Next, a transition to the frequency domain is performed, which is justified as a significant part of practical control engineering is conducted in that domain. For assumed specific plant structures, both ADRC and IDRC are then holistically compared in terms of transfer function representation and frequency characteristics, as well as steady-state convergence conditions. Such a juxtaposition helps to highlight the similarities and differences of both approaches, whereas the utilized bandwidth parameterization is shown to bring the control system to the same form, thus indicating some interesting practical aspects. Finally, the theoretical results concerning both considered control structures are validated in a set of numerical simulations and experiments conducted on a laboratory hardware testbed.

Key words: active disturbance rejection control; extended state observer; state feedback control; integral compensator; ball balancing table

1. INTRODUCTION

The disturbance observer-based control has been extensively studied in the scientific literature as an alternative to integral control. In this approach, an observer estimates the disturbance, which is subsequently countered by the control law. This method is grounded in the internal model principle: whereas integral controllers implicitly reconstruct the disturbance through their integral component, disturbance observers explicitly incorporate the disturbance model. Recent reviews [1, 2], along with related references, analyze the vast research area and point to active disturbance rejection control (ADRC) as one of the more prominent approaches.

The ADRC methodology was developed from a firm premise that theoretical concepts must be applicable in real-world scenarios and that meaningful control theory should not merely be an extension of mathematics based on precise mathematical models of physical processes [3]. This manifested itself in the body of work on ADRC that showcased how to design control systems naturally resistant to unmodeled/uncertain dynamics and disturbances [4].

As it recently turned out, ADRC has more in common with standard controllers than initially thought [5, 6]. One can argue that if ADRC methodology is viewed from the perspective of the Gartner Hype Cycle, then it finally reached its *plateau of productivity* stage. It also indicates that the applicability and relevance of ADRC are now better understood and its mainstream adoption took off (based on the recent integration of ADRC by top industry players like Texas Instruments and Mathworks). It seems that the current meaningful development of ADRC has shifted because of that and now goes towards finding connections with classical controllers rather than distancing from them and simply claiming superiority. For one, it was recognized that ADRC is not a single, rigid set of equations; it is an idea of how to look at, analyze, and solve control problems. The ADRC methodology can produce control schemes in different forms, all depending on what is expected from the control solution and what limitations are posed [7, 8].

As an example, there has been increasing interest within the control community to investigate more deeply the structural [9] and parameter [10] similarities between proportional-integral-derivative (PID) controller and ADRC and possibly show a transition formula. A major step towards connecting theory and practice with ADRC and enabling its backward compatibility with classical controllers came with the parameterization of all controller gains based on bandwidth [11]. By integrating ADRC design principles with Bode's and Nyquist's frequency domain concepts and terminology, ADRC has become more accessible to engineers and has frequently become the preferred tool in practical applications. The proposed bandwidth parameterization also enhanced its user-friendliness and positioned it as a practical alternative to PID due to its simplicity, robustness, performance, and ease of tuning. Interestingly, it was demonstrated that, with some simplifications and for low-order systems, ADRC is indeed backward compatible

*e-mail: jacek.michalski@put.poznan.pl

with standard PI [12] and PID [13] controllers when considering first- and second-order plant dynamics, respectively.

The topic of finding equivalences of ADRC with other control approaches led to investigations done for sliding mode control [14], so-called *flat filters* [15], and eventually the standard internal model control [16, 17].

Based on the above, the motivation for this work comes from the need for ADRC to overcome one of its crucial challenges: achieving backward compatibility with classical controllers. As argued in [18], overlooking this challenge arguably caused many established advanced control schools to stagnate and led to doubts about their relevance in practical applications.

Therefore, the goal of this paper is to take another step towards backward compatibility of ADRC. Here, we revisit a particular control approach, namely a classical state-feedback control with integral compensator [19], and investigate the existence of any equivalences between these two approaches. For convenience and brevity, we will denote the classic approach as IDRC. The specific contributions of the paper are:

- derivation of the control system structure with an integrating compensator and a Luenberger observer in a version not overly dependent on the availability of a mathematical model of the governed plant;
- side-by-side comparison of ADRC and IDRC for assumed specific plant structures in terms of transfer function representation, frequency characteristics, and steady-state convergence conditions;
- showing similarities and differences between ADRC and IDRC as well as proposing parameterization bringing both control systems to the same form, thus indicating certain practical aspects;
- and finally validation of theoretical results using simulation and hardware tests conducted on a laboratory ball balancing experimental table.

The rest of the paper is organized as follows. Section 2 recalls some of the key information from existing literature regarding both ADRC and IDRC approaches that will become useful in the course of the subsequent analysis. It also shows what are the general plant model and control objective considered in the paper. Section 3 contains the main results of the work, namely it shows the detailed investigation into the backward compatibility analysis of ADRC and the classic IDRC approaches. Then, in Section 4, validation of the findings is shown using a set of various simulation and experimental tests. Finally, Section 5 concludes the work.

2. PREREQUISITES

2.1. General plant model and control objective

Consider a dynamical system of n^{th} order, described by the following differential equation

$$y^{(n)} = -a_{n-1}y^{(n-1)} - \ldots - a_1\dot{y} - a_0 y + d + g(\cdot) + bu, \qquad (1)$$

where $y = y(t)$ is the output signal, $y^{(n)} = y^{(n)}(t)$ is the n^{th} time derivative of the output, $u = u(t)$ is the control signal, b is the input gain scaling factor, $d = d(t)$ is the external disturbance, $g(\cdot) = g(y, \ldots, y^{(n-1)}, u, t)$ is the function containing system nonlinearities and unmodeling dynamics part, and $a_i \in \mathbb{R}$ are parameters describing the linear part of the system dynamics (characteristic polynomial coefficients).

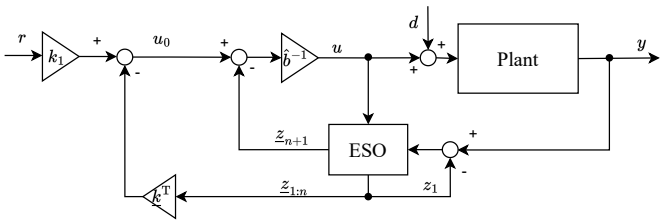

Fig. 1. Block diagram of the considered ADRC structure

Let us rewrite the dynamics Eq. (1) assuming that parameters a_i and terms d and $g(\cdot)$ are unknown and that the value of the input gain b is replaced by its estimate $\hat{b}$. In such a case, one can define a total disturbance of the system Eq. (1) as:

$$f(\cdot) = -a_{n-1}y^{(n-1)} - \ldots - a_1\dot{y} - a_0 y + d + g(\cdot) + (b - \hat{b})u. \quad (2)$$

Taking advantage of the total disturbance, one can put dynamics Eq. (1) into the following form

$$y^{(n)} = \hat{b}u + f(\cdot). \qquad (3)$$

The state-space representation of the system Eq. (3) in the canonical form can be described by

$$\begin{cases} \dot{\underline{x}} = \mathbf{A}\underline{x} + \hat{b}\underline{b}u + \underline{h}f(\cdot), \\ y = \underline{c}^{\mathrm{T}}\underline{x}, \end{cases} \qquad (4)$$

where the state of the system is considered in the phase configuration $\underline{x} = [x_1, x_2, \ldots, x_n]^{\mathrm{T}} = [y, \dot{y}, \ldots, y^{(n-1)}]^{\mathrm{T}}$ and matrices in Eq. (4) are given as

$$\mathbf{A} = \begin{bmatrix} 0 & 1 & 0 & \cdots & 0 \\ 0 & 0 & 1 & \cdots & 0 \\ \vdots & \vdots & \vdots & \ddots & \vdots \\ 0 & 0 & 0 & \cdots & 1 \\ 0 & 0 & 0 & \cdots & 0 \end{bmatrix}, \underline{b} = \begin{bmatrix} 0 \\ 0 \\ \vdots \\ 0 \\ 1 \end{bmatrix}, \underline{h} = \begin{bmatrix} 0 \\ 0 \\ \vdots \\ 0 \\ 1 \end{bmatrix}, \underline{c} = \begin{bmatrix} 1 \\ 0 \\ \vdots \\ 0 \\ 0 \end{bmatrix}.$$

In this work, the control task is to stabilize the output y of the system (4) at the constant reference value $r = \text{const}$. Therefore, derivatives of the reference signal are not considered ($\dot{r} = \ldots = r^{(n)} = 0$). The occurrence of the feedforward part in the presented control laws is also not assumed.

2.2. ADRC

For ADRC control, an extended state observer (ESO) that estimates the state of the plan and a total disturbance is an essential component, which is used in the decoupling loop to actively reject a disturbance. Next, the external control loop is designed for the decoupled system. The idea of ADRC operation is given in Fig. 1.

The main assumption of the ADRC approach is to shape the dynamics of the control plant to approximately match the following integral chain model

$$y^{(n)} = u_0, \qquad (5)$$

Comparing the desired system dynamics Eq. (5) and the control plant model Eq. (3), one can obtain the general control law dependent on the new control signal

$$u = \frac{1}{\hat{b}}(u_0 - f(\cdot)). \tag{6}$$

Assuming the extended state vector $\underline{x}_e = [\underline{x}^{\mathrm{T}}, f(\cdot)]^{\mathrm{T}} \in \mathbb{R}^{n+1}$, the extended state-space representation of model Eq. (4), used in the control system synthesis, can be described as follows

$$\begin{cases} \dot{\underline{x}}_e = \mathbf{A}_e \underline{x}_e + \hat{b}\underline{b}_e u + \underline{h}_e \dot{f}, \\ y = \underline{c}_e^{\mathrm{T}} \underline{x}_e, \end{cases} \tag{7}$$

where

$$\mathbf{A}_e = \begin{bmatrix} \mathbf{A} & \underline{b} \\ \underline{0}_{1\times n} & 0 \end{bmatrix}, \underline{b}_e = \begin{bmatrix} \underline{b} \\ 0 \end{bmatrix}, \underline{c}_e = \begin{bmatrix} \underline{c} \\ 0 \end{bmatrix}, \underline{h}_e = \begin{bmatrix} \underline{h} \\ 0 \end{bmatrix}.$$

For the state estimation process, the following Luenberger-based observer is used

$$\dot{\underline{z}}_e = \left(\mathbf{A}_e - \underline{l}_e \underline{c}_e^{\mathrm{T}}\right) \underline{z}_e + \underline{b}_e \hat{b} u + \underline{l}_e y, \tag{8}$$

where $\underline{z}_e^{\mathrm{T}} = [z_1, z_2, ..., z_n, z_{n+1}] = [\hat{y}, \hat{\dot{y}}, ..., \hat{y}^{(n-1)}, \hat{f}(\cdot)]$ is the estimated state vector and $\underline{l}_e = [l_1, l_2, ..., l_{n+1}]^{\mathrm{T}}$ represents the gains of the ESO.

To stabilize the plant output at constant value r one can use the estimated state vector $\underline{z}$ in control law Eq. (6). Assuming that gains of the observer Eq. (8) are selected such that the estimation error is $\left\|\underline{z}_e - \underline{x}_e\right\| < \varepsilon$, where $\varepsilon > 0$ is some positive constant small enough, one can apply the following control law

$$u_0 = k_1 r - \underline{k}^{\mathrm{T}} \underline{z}_{e,1:n}, \tag{9}$$

where $\underline{k}^{\mathrm{T}} = [k_1, k_2, ..., k_n]$. Thus, combining Eq. (9) and Eq. (6), one obtains the final form of the control law as

$$u = \frac{1}{\hat{b}}(u_0 - z_{e,n+1}) = \frac{1}{\hat{b}}\left(k_1 r - \underline{k}_e^{\mathrm{T}} \underline{z}_e\right), \tag{10}$$

with $\underline{k}_e^{\mathrm{T}} = [k^{\mathrm{T}}, 1]$.

Parameterization of ESO and controller

The ESO gains vector $\underline{l}_e$ and the controller gains vector $\underline{k}$ are selected such that the eigenvalues of the observer and closed-loop system matrix are equal to the desired parameters. Here, a design based on the separation principle is used which is a key ingredient in the ADRC design. To be more precise, gains satisfy the following relationships

$$\begin{aligned} \det\left(s\mathbf{I} - \left(\mathbf{A}_e - \underline{l}_e \underline{c}_e^{\mathrm{T}}\right)\right) &= \varphi_o^{\mathrm{ADRC}}(s), \\ \det\left(s\mathbf{I} - \left(\mathbf{A}_p - \underline{b}_P \underline{k}^{\mathrm{T}}\right)\right) &= \varphi_c^{\mathrm{ADRC}}(s), \end{aligned} \tag{11}$$

where $\mathbf{I}$ is the identity matrix, $\varphi_c^{\mathrm{ADRC}}(s)$ and $\varphi_o^{\mathrm{ADRC}}(s)$ stand for the assumed Hurwitz-stable polynomials. To facilitate the selection of these polynomials, one can employ a simple pole placement method, commonly used in ADRC design [11], represented by the following formulas

$$\varphi_o^{\mathrm{ADRC}}(s) = (s+\omega_o)^{n+1}, \quad \varphi_c^{\mathrm{ADRC}}(s) = (s+\omega_c)^n, \tag{12}$$

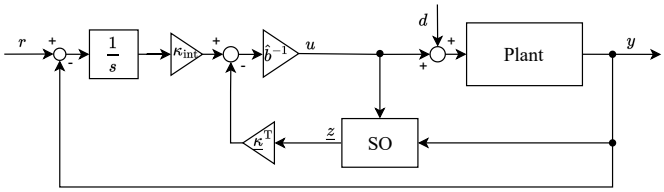

Fig. 2. Block diagram of the considered IDRC structure

where ω_o and ω_c are observer and controller bandwidths, respectively. Combining (12) and (11), one respectively gets

$$\mathrm{eig}_i\left[\mathbf{A}_e - \underline{l}_e \underline{c}_e^{\mathrm{T}}\right] = -\omega_o \quad \text{for} \quad i = 1,2,...,n+1, \tag{13}$$

$$\mathrm{eig}_j\left[\mathbf{A}_p - \underline{b}_P \underline{k}^{\mathrm{T}}\right] = -\omega_c \quad \text{for} \quad j = 1,2,...,n, \tag{14}$$

where $\mathrm{eig}_\zeta(\cdot)$ means the ζ-th eigenvalue of the given matrix. The solution to (13) and (14) can be briefly specified as

$$l_i = \binom{n+1}{i} \omega_{\mathrm{o}}^i, \quad k_j = \binom{n}{j-1} \omega_{\mathrm{c}}^{n-j+1}, \tag{15}$$

where $\binom{v}{m} = \frac{v!}{m!(v-m)!}$ stands for binomial coefficients.

2.3. IDRC

The IDRC combines classical state-feedback control with integral compensator [19], along with specific assumptions regarding the system model. Similarly to ADRC, it is assumed that the system dynamics (characteristic polynomial and nonlinear components from Eq. (1)) are generally unknown. Synthesis of the algorithm is based on preliminary knowledge about the system dynamics order and input gain coefficient. The sctructure of the IDR controller is presented in Fig. 2.

In this approach, it is assumed that the system dynamics is represented by Eq. (4). It is worth noting that, unlike in ADRC, an estimate of the total disturbance function from Eq. (4) is not used in the IDRC controller synthesis. A detailed explanation is provided in Section 3.

Employing the Luenberger state observer (SO) to estimate the state of the system Eq. (4) the formula is obtained

$$\dot{\underline{z}} = \left(\mathbf{A} - \underline{\iota}\underline{c}^{\mathrm{T}}\right) \underline{z} + \underline{b}\hat{b} u + \underline{\iota} y, \tag{16}$$

where the observer state vector $\underline{z}$ consists of $\underline{z} = [z_1, z_2, ..., z_n]^{\mathrm{T}} = [\hat{y}, \hat{\dot{y}}, ..., \hat{y}^{(n-1)}]^{\mathrm{T}}$ and $\underline{\iota} = [\iota_1, \iota_2, ..., \iota_n]^{\mathrm{T}}$ contains set of observer gains.

The control law for constant value control is defined as state feedback with an integral action to compensate the steady-state error and constant external disturbances

$$u = \frac{1}{\hat{b}}\left(-\underline{\kappa}^{\mathrm{T}} \underline{z} + \kappa_{\mathrm{int}} \int_0^t (r(\tau) - y(\tau)) d\tau\right), \tag{17}$$

where $\underline{\kappa}^{\mathrm{T}} = [\kappa_1, \kappa_2, ..., \kappa_n]$ and the κ_{int} term is an integral path gain. Assuming that $\underline{z} \approx \underline{x}$ and substituting control law into model Eq. (4) leads to following closed-loop dynamics

$$\dot{\underline{x}} = \mathbf{A}\underline{x} - \underline{b}\underline{\kappa}^{\mathrm{T}} \underline{x} + \underline{b}\kappa_{\mathrm{int}} \int_0^t (r(\tau) - y(\tau)) d\tau, \tag{18}$$

then extending the state vector $\underline{x}$ by integral of control error

$q = \int_0^t (r(\tau) - y(\tau))d\tau$ gives the form

$$\begin{bmatrix} \underline{\dot{x}} \\ \dot{q} \end{bmatrix} = \underbrace{\begin{bmatrix} \mathbf{A} - \underline{b}\underline{\kappa}^{\mathrm{T}} & \underline{b}\kappa_{\mathrm{int}} \\ -\underline{c}^{\mathrm{T}} & 0 \end{bmatrix}}_{\mathbf{H}_{\mathrm{CL}}^{\mathrm{IDRC}}} \begin{bmatrix} \underline{x} \\ q \end{bmatrix} + \begin{bmatrix} \underline{0} \\ 1 \end{bmatrix} r, \tag{19}$$

where r is the reference value for the closed-loop system.

Preliminary parameterization of SO and controller

Following the commonly used parameterization for ADRC, we apply it to the IDRC structure. Similarly, we separate the feedback and observer design and consider the following

$$\begin{aligned} \det\left(s\mathbf{I} - \left(\mathbf{A} - \underline{\iota}\underline{c}^{\mathrm{T}}\right)\right) &= \varphi_o^{\mathrm{IDRC}}(s), \\ \det\left(s\mathbf{I} - \mathbf{H}_{\mathrm{CL}}^{\mathrm{IDRC}}\right) &= \varphi_c^{\mathrm{IDRC}}(s), \end{aligned} \tag{20}$$

with $\varphi_c^{\mathrm{IDRC}}(s)$ and $\varphi_o^{\mathrm{IDRC}}(s)$ being the assumed Hurwitz-stable polynomials. Similarly as in ADRC, one can use parameters ω_c and ω_c to tune the feedback and observer bandwidths, respectively. In this case one assumes

$$\varphi_o^{\mathrm{IDRC}}(s) = (s+\omega_o)^n, \quad \varphi_c^{\mathrm{IDRC}}(s) = (s+\omega_c)^{n+1}, \tag{21}$$

from which it follows that

$$\mathrm{eig}_i\left[\mathbf{A} - \underline{\iota}\underline{c}^{\mathrm{T}}\right] = -\omega_o \quad \text{for} \quad i = 1,2,\ldots,n, \tag{22}$$

$$\mathrm{eig}_j\left[\mathbf{H}_{\mathrm{CL}}\right] = -\omega_c \quad \text{for} \quad j = 1,2,\ldots,n+1. \tag{23}$$

The SO and controller gains satisfying Eq. (22)-(23) can be obtained using Newton's binomial form as

$$\iota_i = \binom{n}{i}\omega_{\mathrm{o}}^i, \quad \kappa_j = \binom{n+1}{j-1}\omega_{\mathrm{c}}^{n-j+2}. \tag{24}$$

Moreover, according to Eq. (19), κ_j obtained from Eq. (24) the form of extended controller gains vector $[\underline{\kappa}^{\mathrm{T}}, \kappa_{\mathrm{int}}]^{\mathrm{T}}$, where $\underline{\kappa}^{\mathrm{T}}$ is the state feedback vector consisting of κ_j gains for $j = 2,3,\ldots,n+1$ and κ_{int} is the integral path gain such that $\kappa_{\mathrm{int}} = \kappa_j$ for $j = 1$.

Remark 1. *Due to the assumption that the plant is subject to modeling uncertainties, the selection of settings is heuristic. The bandwidth values are selected to obtain the desired properties of the closed-loop system (the desired speed or sensitivity to noises), and some of its features will be visible in the transfer function notation presented in the next section. In addition, the range of parameter values that ensure stable system operation depends on the structure and parameters of the plant.*

Examples of the influence of ADRC parameters on the operation of the control system can be found in detail in [20]. Studies on the influence of uncertainty of selected parameters on the control quality can be found in [21, 22].

3. THEORETICAL ANALYSIS OF ADRC AND IDRC

This section compares ADRC and IDRC approaches in various aspects. The steady-state convergence (conditions to eliminate the steady-state error and compensating the external disturbances) are analyzed. Transfer function representations are derived and tuning parameterizations are proposed.

The main difference between ADRC and IDRC lies in the method of extending the system state. In ADRC, the state is extended due to the observer structure, whereas in IDRC, the state extension occurs within the controller.

Remark 2. *It is noteworthy that in the IDRC approach, the total disturbance $f(\cdot)$ present in the model in Eq. (7) is not explicitly taken into account in the controller synthesis process. However, in this approach, disturbance rejection is embedded within the controller loop and lacks a direct interpretation as in the classic ADRC approach. Thus, the employed Luenberger observer in Eq. (16) does not have the extended state variable representing the estimate of the total disturbance. Implications of non-extended state estimation is discussed in section 3.1.*

Remark 3. *According to obtained control laws in both algorithms, in IDRC approach Eq. (17) the $k_1 r$ term is not required as in ADRC Eq. (10), because incorporating an integral compensator ensures the unit static gain of the closed-loop system.*

3.1. Steady-state convergence analysis in ADRC and IDRC

The considerations in this section are conducted under the following assumptions:

- closed-loop system is asymptotically stable for both structures and the influence of external disturbance is considered after the transition process due to the reference signal;
- input gain coefficient b is known and used in the synthesis of both algorithms ($\hat{b} = b$);
- ESO and controller gains $\underline{l}_e$, $\underline{k}^{\mathrm{T}}$ in ADRC are selected with respect to Eq. (15);
- observer and controller gains $\underline{\iota}$, $[\underline{\kappa}^{\mathrm{T}}, \kappa_{\mathrm{int}}]^{\mathrm{T}}$ in IDRC are selected with respect to Eq. (24).

To facilitate the analysis, the following linear model of the external disturbance (uncorrelated with the system state) is taken into account

$$d = \varepsilon t + \xi, \tag{25}$$

where ε and ξ are constant (coefficients of the linear equation).

ADRC

Dynamics of estimation error $\underline{e}_o = \underline{x}_e - \underline{z}_e$ under influence of external disturbance from Eq. (25) in ADRC approach is

$$\dot{\underline{e}}_o = \left(\mathbf{A}_e - \underline{\iota}\underline{c}_e^{\mathrm{T}}\right)\underline{e}_o + \underline{h}_e\dot{d}, \tag{26}$$

thus, since $\mathbf{H}_o = \left(\mathbf{A}_e - \underline{\iota}\underline{c}_e^{\mathrm{T}}\right)$ is a Hurwitz matrix, the norm of estimation errors converge to a constant for any constant $\dot{d}$ and zero for any constant d. In particular, the estimation error $\underline{e}_o$ caused by constant $\dot{d}$ can be obtained using the final value theorem in s domain

$$\underline{E}_o(s) = \left(s\mathbf{I} - \mathbf{H}_o\right)^{-1}\left(\underline{h}_e s D(s)\right), \tag{27}$$

thus

$$\underline{e}_o(\infty) = \lim_{s\to 0} s\underline{E}_o(s) = -\mathbf{H}_o^{-1}\lim_{s\to 0}\left(\underline{h}_e s^2 D(s)\right). \tag{28}$$

Substituting the control law Eq. (10) (with biased extended state estimates) in the system model Eq. (4) leads to

$$\dot{\underline{x}} = \underbrace{\left(\mathbf{A} - \underline{b}k^{\mathrm{T}}\right)}_{\mathbf{H}_{\mathrm{CL}}^{\mathrm{ADRC}}} \underline{x} + \underline{b}k^{\mathrm{T}}\underline{e}_{o,1:n} + \underbrace{\underline{h}\left(d - \hat{d}\right)}_{e_{o,n+1}} + \underline{b}k_1 r. \tag{29}$$

The limit value of state $\underline{x}$ can be easily obtained as in Eq. (28)

$$\underline{x}(\infty) = \lim_{s\to 0} s\underline{X}(s) = -(\mathbf{H}_{\mathrm{CL}}^{\mathrm{ADRC}})^{-1}\left(\underline{b}k^{\mathrm{T}} s\underline{E}_{o,1:n}(s) + \right. \\ \left. + \underline{h} s\underline{E}_{o,n+1}(s) + \underline{b}k_1 sR(s)\right). \tag{30}$$

Example 1. *Taking advantage of Eq. (28), the final estimation error for the disturbance Eq. (25) can be derived*

$$\underline{e}_o(\infty) = \varepsilon \begin{bmatrix} \frac{1}{\omega_o^{n+1}} & \binom{n+1}{1}\frac{1}{\omega_o^n} & \binom{n+1}{2}\frac{1}{\omega_o^{n-1}} & \cdots & \binom{n+1}{n}\frac{1}{\omega_o} \end{bmatrix}^T. \tag{31}$$

This result indicates that in the limit, components of $\underline{e}_o$ are constant. Next, substituting the Laplace transform of $\underline{e}_o$ in Eq. (30) one obtains

$$\underline{x}(\infty) = \begin{bmatrix} y(\infty) \\ \dot{y}(\infty) \\ \ddot{y}(\infty) \\ \vdots \\ y^{(n-1)}(\infty) \end{bmatrix} = \begin{bmatrix} r + \frac{\varepsilon}{\omega_c^{n+1}} \sum_{i=1}^{n+1} \binom{n}{i-1}\binom{n+1}{i}\left(\frac{\omega_c}{\omega_o}\right)^i \\ 0 \\ \vdots \\ 0 \end{bmatrix}, \tag{32}$$

which shows a non-zero control error in steady state.

IDRC

In the IDRC approach, the dynamics of estimation error $\underline{e}_o = \underline{x} - \underline{z}$ is described by

$$\dot{\underline{e}}_o = \left(\mathbf{A} - \underline{\iota}\underline{c}^{\mathrm{T}}\right)\underline{e}_o + \underline{h}d. \tag{33}$$

Since the observer state matrix $\mathbf{H}_o = \left(\mathbf{A} - \underline{\iota}\underline{c}^{\mathrm{T}}\right)$ is Hurwitz, the norm of state estimation error $\underline{e}_o$ converges to a constant for any constant d. It can be derived from Eq. (33), that the derivative of estimation error yields

$$\dot{\underline{e}}_o(\infty) = \lim_{s\to 0} s^2\underline{E}_o(s) = -\mathbf{H}_o^{-1}\lim_{s\to 0}\left(\underline{h}_e s^2 D(s)\right). \tag{34}$$

Applying the control law Eq. (17) with biased state estimates $\underline{z}$ to dynamics of the model Eq. (4) gives the following

$$\dot{\underline{x}} = \mathbf{A}\underline{x} - \underline{b}k^{\mathrm{T}}\underline{x} + \underline{b}\kappa_{\mathrm{int}}\int_0^t (r(\tau) - y(\tau))d\tau + \underline{b}\underline{\kappa}^{\mathrm{T}}\underline{e}_o + \underline{h}d, \tag{35}$$

and describing the dynamics Eq. (35) by extension of system state vector as in Eq. (19) leads to the form

$$\begin{bmatrix} \dot{\underline{x}} \\ \dot{q} \end{bmatrix} = \underbrace{\begin{bmatrix} \mathbf{A} - \underline{b}\underline{\kappa}^{\mathrm{T}} & \underline{b}\kappa_{\mathrm{int}} \\ -\underline{c}^{\mathrm{T}} & 0 \end{bmatrix}}_{\mathbf{H}_{\mathrm{CL}}^{\mathrm{IDRC}}} \begin{bmatrix} \underline{x} \\ q \end{bmatrix} + \\ + \begin{bmatrix} \underline{b}\underline{\kappa}^{\mathrm{T}} & 0 \\ \underline{0} & 0 \end{bmatrix}\begin{bmatrix} \underline{e}_o \\ 0 \end{bmatrix} + \begin{bmatrix} \underline{h} \\ 0 \end{bmatrix} d + \begin{bmatrix} \underline{0} \\ 1 \end{bmatrix} r. \tag{36}$$

Based on the state vector configuration in Eq. (36), the q variable represents the integral of the control error $r - y$. There is a need to differentiate that equation to calculate the final value of the state vector possible, which consists of the control error.

$$\underbrace{\begin{bmatrix} \dot{\underline{x}} \\ \ddot{q} \end{bmatrix}}_{\dot{\underline{x}}^*} = \mathbf{H}_{\mathrm{CL}}^{\mathrm{IDRC}} \underbrace{\begin{bmatrix} \underline{x} \\ \dot{q} \end{bmatrix}}_{\underline{x}^*} + \begin{bmatrix} \underline{b}\underline{\kappa}^{\mathrm{T}} & \underline{0} \\ \underline{0}^{\mathrm{T}} & 0 \end{bmatrix}\begin{bmatrix} \dot{\underline{e}}_o \\ 0 \end{bmatrix} + \begin{bmatrix} \underline{h} \\ 0 \end{bmatrix}\dot{d} + \begin{bmatrix} \underline{0} \\ 1 \end{bmatrix}\dot{r}. \tag{37}$$

Thus, applying the final value theorem in Eq. (37) leads to

$$\underline{x}^*(\infty) = \lim_{s\to 0} s\underline{X}^*(s) = -(\mathbf{H}_{\mathrm{CL}}^{\mathrm{IDRC}})^{-1}\lim_{s\to 0} \\ \left(\begin{bmatrix} \underline{b}k^{\mathrm{T}} & \underline{0} \\ \underline{0} & 0 \end{bmatrix}\begin{bmatrix} s^2\underline{E}_o(s) \\ 0 \end{bmatrix} + \begin{bmatrix} \underline{h} \\ 0 \end{bmatrix} s^2 D(s) + \begin{bmatrix} \underline{0} \\ 1 \end{bmatrix} s^2 R(s)\right). \tag{38}$$

Example 2. *Similarly to ADRC, the estimation error for the disturbance Eq. (25) in the IDRC can be considered. Using Eq. (34) one obtains*

$$\dot{\underline{e}}_o(\infty) = \varepsilon \begin{bmatrix} \frac{1}{\omega_o^n} & \binom{n}{1}\frac{1}{\omega_o^{n-1}} & \binom{n}{2}\frac{1}{\omega_o^{n-2}} & \cdots & \binom{n}{n-1}\frac{1}{\omega_o} \end{bmatrix}^T. \tag{39}$$

It can be seen that the derivative vector of estimation error $\dot{\underline{e}}_o$ is constant. Substituting the Laplace transform of Eq. (39) into Eq. (38) leads to the final value of the assumed state vector

$$\underline{x}^*(\infty) = \begin{bmatrix} \dot{y}(\infty) \\ \ddot{y}(\infty) \\ \vdots \\ y^{(n)} \\ e_c(\infty) \end{bmatrix} = \begin{bmatrix} 0 \\ 0 \\ \vdots \\ 0 \\ -\frac{\varepsilon}{\omega_c^{n+1}} \sum_{i=1}^{n+1} \binom{n}{i-1}\binom{n+1}{n+2-i}\left(\frac{\omega_c}{\omega_o}\right)^{i-1} \end{bmatrix}. \tag{40}$$

The most important conclusion is that despite the conflicting convergence conditions of state estimation, the convergence of the control error to zero in both methods requires that d be a constant value. In ADRC, the convergence of the control error is conditioned by the quality (consistency) of estimation. It can also be concluded that the ESO bandwidth ω_o has a crucial impact in attenuation of steady-state control error, while in IDRC approach this role is more divided into observer and controller, which can be noted by comparing the exponents of observer and controller bandwidth ω_o, ω_c in Eqs. (32), (40). For assumed $\omega_o = \omega_c$ as the result of Proof 1, it can be seen that the steady-state convergence conditions will be equivalent for both the ADRC and IDRC approaches. Convergence conditions for estimation and control error are summarized in Table 1.

Table 1. Convergence conditions for estimation and control error

Requirement	Condition for ADRC	Condition for IDRC
$\underline{e}_o = 0$	$d = \mathrm{const}$	$d = 0$
$\underline{e}_o = \mathrm{const}$	$\dot{d} = \mathrm{const}$	$d = \mathrm{const}$
$e_c(\infty) = 0$	$\underline{e}_o = 0$	$\underline{e}_o = \mathrm{const}$

3.2. Transfer function analysis

Transfer function analysis can be performed for the linear (or linearized) part of the model of the system. According to the general system introduced in section 2.1, under assumption

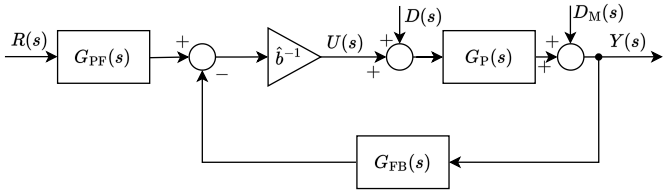

Fig. 3. Block diagram of considered control loop

that $d = 0$, $g(\cdot) = 0$ and $\hat{b} = b$, the following transfer function that describes linear dynamics of Eq. (1) can be investigated

$$G_p(s) = \frac{Y(s)}{U(s)}\bigg|_{d=0,g(\cdot)=0} = \frac{b}{s^n + a_{n-1}s^{n-1} + \ldots + a_0}. \quad (41)$$

To provide the transfer analysis for general model of the system Eq. (41), there is a need to determine the model of the linear part of the system dynamics, which state-space representation is similar to (4), but has different form of state matrix:

$$\mathbf{A}^* = \begin{bmatrix} 0 & 1 & 0 & \cdots & 0 \\ 0 & 0 & 1 & \cdots & 0 \\ \vdots & \vdots & \vdots & \ddots & \vdots \\ 0 & 0 & 0 & \cdots & 1 \\ -a_0 & -a_1 & -a_2 & \cdots & -a_{n-1} \end{bmatrix},$$

which will be used in further theoretical derivations and considerations (to determine the plant transfer function $G_p(s)$).

In the description from Eq. (4), according to ADRC methodology, it is assumed that the model of the system is highly uncertain. So, even its linear part is treated as a part of total disturbance $f(\cdot)$, thus the state matrix contains only zeros in last row.

However, closed-loop transfer function analysis requires knowledge about the system model, and for further derivations, $\mathbf{A}^*$ will be used as a state matrix of the system.

The analysis began with a comparison of the transfer function equivalents of the controller in the ADRC and IDRC approaches. For this purpose, the $G_{\mathrm{PF}}(s)$ and $G_{\mathrm{FB}}(s)$ (its interpretation can be found in Fig. 3) transfer functions were calculated below in both approaches for the most commonly assumed order of the plant dynamics n in the synthesis of the algorithm.

Transfer function derivations in ADRC

Rewriting the state-space equations of the ESO dynamics Eq. (8) and combining it with the control law Eq. (10) (constant value control)

$$\begin{cases} \dot{\underline{z}}_e = \left(\mathbf{A}_e - \underline{l}_e \underline{c}_e^{\mathrm{T}}\right)\underline{z}_e + \underline{b}_e \hat{b} u + \underline{l}_e y, \\ u = \frac{1}{\hat{b}}\left(k_1 r - \underline{k}_e^{\mathrm{T}} \underline{z}_e\right), \end{cases} \quad (42)$$

where $\underline{k}_e = [\underline{k}^{\mathrm{T}}, 1]^{\mathrm{T}}$ is the extended vector of the controller gains which makes it possible to combine the state feedback and disturbance rejection loop. Then, substituting the control law into the ESO equations Eq. (42) leads to the expression

$$\dot{\underline{z}}_e = \underbrace{\left(\mathbf{A}_e - \underline{l}_e \underline{c}_e^{\mathrm{T}} - \underline{b}_e \underline{k}_e^{\mathrm{T}}\right)}_{\mathbf{A}_{\mathrm{CL}}^{\mathrm{ADRC}}} \underline{z} + \underline{\iota} y + k_1 \underline{b}_e r. \quad (43)$$

Applying the Laplace transform to both Eq. (42), Eq. (43) leads to the form

$$\begin{cases} \underline{Z}_e(s) = \left(s\mathbf{I} - \mathbf{A}_{\mathrm{CL}}^{\mathrm{ADRC}}\right)^{-1}\left(\underline{\iota} Y(s) + k_1 \underline{b}_e R(s)\right), \\ U(s) = \frac{1}{\hat{b}}\left(-\underline{k}_e^{\mathrm{T}} \underline{Z}_e(s) + k_1 R(s)\right), \end{cases} \quad (44)$$

and substituting the state estimate vector $\underline{Z}(s)$ to control law in s domain gives its final form

$$U(s) = \overbrace{\frac{1}{\hat{b}} \frac{k_1\left(\det\left(s\mathbf{I} - \mathbf{A}_{\mathrm{CL}}^{\mathrm{ADRC}}\right) - \underline{k}_e^{\mathrm{T}} \mathrm{adj}\left(s\mathbf{I} - \mathbf{A}_{\mathrm{CL}}^{\mathrm{ADRC}}\right)\underline{b}_e\right)}{\det\left(s\mathbf{I} - \mathbf{A}_{\mathrm{CL}}^{\mathrm{ADRC}}\right)}}^{G_{\mathrm{PF}}(s)} R(s) + \underbrace{-\frac{1}{\hat{b}} \frac{\underline{k}_e^{\mathrm{T}} \mathrm{adj}\left(s\mathbf{I} - \mathbf{A}_{\mathrm{CL}}^{\mathrm{ADRC}}\right)\underline{\iota}}{\det\left(s\mathbf{I} - \mathbf{A}_{\mathrm{CL}}^{\mathrm{ADRC}}\right)}}_{G_{\mathrm{FB}}(s)} Y(s). \quad (45)$$

Transfer function derivations in IDRC

Rewriting the state-space equations Eq. (16) of the SO dynamics and assumed formula for constant value control Eq. (17)

$$\begin{cases} \dot{\underline{z}} = \left(\mathbf{A} - \underline{\iota} \underline{c}^{\mathrm{T}}\right)\underline{z} + \underline{b}\hat{b} u + \underline{\iota} y, \\ u = \frac{1}{\hat{b}}\left(-\underline{\kappa}^{\mathrm{T}} \underline{z} + \kappa_{\mathrm{int}} \int_0^t (r(\tau) - y(\tau)) d\tau\right), \end{cases} \quad (46)$$

then substituting the control law u into the SO Eq. (46) results in the following

$$\dot{\underline{z}} = \underbrace{\left(\mathbf{A} - \underline{\iota} \underline{c}^{\mathrm{T}} - \underline{b}\underline{\kappa}^{\mathrm{T}}\right)}_{\mathbf{A}_{\mathrm{CL}}^{\mathrm{IDRC}}} \underline{z} + \underline{b}\kappa_{\mathrm{int}} \int_0^t (r(\tau) - y(\tau)) d\tau + \underline{\iota} y. \quad (47)$$

Applying the Laplace transform for both Eq. (46), Eq. (47) leads to the form

$$\begin{cases} \underline{Z}(s) = \left(s\mathbf{I} - \mathbf{A}_{\mathrm{CL}}^{\mathrm{IDRC}}\right)^{-1}\left(\left(\underline{\iota} - \underline{b}\frac{\kappa_{\mathrm{int}}}{s}\right) Y(s) + \underline{b}\frac{\kappa_{\mathrm{int}}}{s} R(s)\right), \\ U(s) = \frac{1}{\hat{b}}\left(-\underline{\kappa} \underline{Z}(s) + \frac{\kappa_{\mathrm{int}}}{s} R(s) - \frac{\kappa_{\mathrm{int}}}{s} Y(s)\right), \end{cases} \quad (48)$$

and substituting the state estimate vector $\underline{Z}(s)$ to control law in s domain ensures its final form

$$U(s) = \overbrace{\frac{1}{\hat{b}} \frac{\kappa_{\mathrm{int}}\left(s \det\left(s\mathbf{I} - \mathbf{A}_{\mathrm{CL}}^{\mathrm{IDRC}}\right) - \underline{\kappa}^{\mathrm{T}} \mathrm{adj}\left(s\mathbf{I} - \mathbf{A}_{\mathrm{CL}}^{\mathrm{IDRC}}\right)\underline{b}\right)}{s \det\left(s\mathbf{I} - \mathbf{A}_{\mathrm{CL}}^{\mathrm{IDRC}}\right)}}^{G_{\mathrm{PF}}(s)} R(s) + \underbrace{-\frac{1}{\hat{b}} \frac{\underline{\kappa}^{\mathrm{T}} \mathrm{adj}\left(s\mathbf{I} - \mathbf{A}_{\mathrm{CL}}^{\mathrm{IDRC}}\right)\left(s\underline{\iota} + \underline{b}\kappa_{\mathrm{int}}\right) + \kappa_{\mathrm{int}}\left(\det\left(s\mathbf{I} - \mathbf{A}_{\mathrm{CL}}^{\mathrm{IDRC}}\right)\right.}{s \det\left(s\mathbf{I} - \mathbf{A}_{\mathrm{CL}}^{\mathrm{IDRC}}\right)}}_{G_{\mathrm{FB}}(s)} Y(s). \quad (49)$$

Comparison conditions of the presented approaches

Based on Eq. (45) and Eq. (49), in general case (for assumed n-th order of system dynamics) it can be derived that

$$\begin{aligned} &\varphi^{\mathrm{ADRC}}(s) = \det\left(s\mathbf{I} - \mathbf{A}_{\mathrm{CL}}^{\mathrm{ADRC}}\right) = \\ &= s^{n+1} + \textstyle\sum_{i=1}^{n}\left(k_{n-i+1} + l_i + \sum_{j=1}^{i-1} k_{n-j+1} l_{i-j}\right) s^{n-i+1}, \end{aligned} \quad (50)$$

$$\begin{aligned} &\varphi^{\mathrm{IDRC}}(s) = s\,\det\left(s\mathbf{I} - \mathbf{A}_{\mathrm{CL}}^{\mathrm{IDRC}}\right) = \\ &= s^{n+1} + \textstyle\sum_{i=1}^{n}\left(\kappa_{n-i+1} + \iota_i + \sum_{j=1}^{i-1} \kappa_{n-j+1} \iota_{i-j}\right) s^{n-i+1}. \end{aligned} \quad (51)$$

Moreover, prefilter (PF) and feedback (FB) transfer functions satisfy:

$$G_{\mathrm{PF}}^{\mathrm{ADRC}}(s) = \frac{k_1\left(s^{n+1}+\sum_{i=0}^{n} l_{n+1-i}s^i\right)}{\varphi^{\mathrm{ADRC}}(s)} = k_1\frac{\varphi_o^{\mathrm{ADRC}}(s)}{\varphi^{\mathrm{ADRC}}(s)}, \quad (52)$$

$$G_{\mathrm{PF}}^{\mathrm{IDRC}}(s) = \frac{\kappa_{\mathrm{int}}\left(s^{n}+\sum_{i=0}^{n-1} \imath_{n-i}s^i\right)}{\varphi^{\mathrm{IDRC}}(s)} = \kappa_{\mathrm{int}}\frac{\varphi_o^{\mathrm{IDRC}}(s)}{\varphi^{\mathrm{IDRC}}(s)}, \quad (53)$$

$$G_{\mathrm{FB}}^{\mathrm{ADRC}}(s) = \frac{l_{n+1}s^n+\sum_{i=0}^{n-1}(\sum_{j=1}^{n-i} k_j l_{i+j})s^{n-i}}{\varphi^{\mathrm{ADRC}}(s)} + \frac{\sum_{j=1}^{n} k_{n-j+1}l_{n+1}s^{n-j}}{\varphi^{\mathrm{ADRC}}(s)}, \quad (54)$$

$$G_{\mathrm{FB}}^{\mathrm{IDRC}}(s) = \frac{\kappa_{\mathrm{int}}s^n+\sum_{i=0}^{n-1}(\sum_{j=1}^{n-i} \kappa_j \imath_{i+j})s^{n-i}+\sum_{j=1}^{n}\kappa_{\mathrm{int}}\imath_j s^{n-j}}{\varphi^{\mathrm{IDRC}}(s)}. \quad (55)$$

To make these formulas clearer and more intuitive, the prefilter transfer functions for both approaches, assuming the most common order of system dynamics, are presented in Tab. 2. The feedback transfer functions are listed in Tab. 3.

According to these transfer functions, it can be noted that the denominators have a similar form for both ADRC and IDRC approaches. This similarity pertains only to the distribution of controller and observer gains. However, for arbitrary gains selection, including the parameterizations given by Eqs. (15) and (24), they are not equal.

The numerators of the prefilter transfer functions represent the characteristic polynomials of the ESO and SO state matrices, respectively Eqs. (11), (20) for any assumed order of system dynamics n. These polynomials are scaled by the k_1 factor in ADRC and κ_{int} factor in IDRC. These are the controller gains responsible for ensuring the unit static gains of the closed-loop system.

In the numerator of feedback transfer functions, the coefficients responsible for system robustness (l_{n+1} gain in the ADRC approach and κ_{int} in the IDRC approach) are distributed analogously with respect to the powers of complex variable s.

We will now consider a particular case of parameterization that ensures a certain equivalence of the transfer functions of both analyzed structures, while generalizing the study reported in [23]. This case is described by the following lemma.

Lemma 1. *Assuming that gains are selected according to parameterizations Eq. (15) and Eq. (24) with*

$$\omega_c = \omega_o = \omega, \quad (56)$$

where $\omega > 0$ is a positive parameter, transfer functions $G_{FB}(s)$ and $G_{PF}(s)$ for ADRC and IDRC control schemes satisfy

$$G_{PF}^{IDRC}(s) = \frac{\omega}{(s+\omega)}G_{PF}^{ADRC}(s), \quad (57)$$

and

$$G_{FB}^{ADRC}(s) = G_{FB}^{IDRC}(s). \quad (58)$$

Proof. In order to guarantee that $\varphi^{\mathrm{IDRC}}(s) = \varphi^{\mathrm{ADRC}}(s)$ the following should be satisfied $\forall i = 1,2,\ldots,n$

$$\kappa_{n-i+1} + \imath_i + \sum_{j=1}^{i-1}\kappa_{n-j+1}\imath_{i-j} = k_{n-i+1} + l_i + \sum_{j=1}^{i-1} k_{n-j+1}l_{i-j}. \quad (59)$$

The solution to (59) is

$$\kappa_{n-i+1} = l_i \text{ and } \imath_i = k_{n-i+1}. \quad (60)$$

Since the numerators of $G_{\mathrm{PF}}^{\mathrm{ADRC}}(s)$ and $G_{\mathrm{PF}}^{\mathrm{IDRC}}(s)$ denoted by $\varphi_o^{\mathrm{ADRC}}$ and $\varphi_o^{\mathrm{IDRC}}$ are polynomials of $n+1$ and n degrees, respectively, one can conclude that

$$\varphi_o^{\mathrm{ADRC}}(s) = (s+\gamma)\,\varphi_o^{\mathrm{IDRC}}(s), \quad (61)$$

where $\gamma \in \mathbb{R}$. As a result, assuming that (60) holds, one can state

$$G_{\mathrm{PF}}^{\mathrm{ADRC}}(s) = \frac{k_1}{\kappa_{\mathrm{int}}}(s+\gamma)\,G_{\mathrm{PF}}^{\mathrm{IDRC}}(s). \quad (62)$$

Recalling that $\kappa_{\mathrm{int}} = l_{n+1}$, it can be easily shown that $G_{\mathrm{FB}}^{\mathrm{ADRC}}(s) = G_{\mathrm{FB}}^{\mathrm{IDRC}}(s)$, which corresponds to Eq. (58).

Now, taking into account the standard parameterization of gains scaled by the parameters ω_c and ω_o according to formulas Eq. (15) and Eq. (24) and recalling Eq. (56) one has $\gamma = \omega$ and $\frac{k_1}{\kappa_{\mathrm{int}}} = \frac{k_1}{l_{n+1}}\omega^{-1}$. Thus, based on Eq. (62) one concludes that Eq. (57) holds.

□

Remark 4. *It is worth emphasizing that the presented analysis is theoretical in nature and demonstrates the conditions under which the transfer functions of the ADRC and IDRC structures are similar employing the parameterizations defined by Eqs. (15) and (24). However, this occurs under the strong assumption (56), which states that the state feedback and the observer are tuned analogously. As a result, this significantly limits the degree of freedom in tuning the entire algorithm, which is typically based on increasing the observer gains independently of the chosen feedback. Thus, in practice, the equivalence described by Eqs. (57) and (58) is not required, and a more advanced tuning approach should be proposed.*

Proposed IDRC parameterization

Here, we will make a more general comparison of both control structures. In order to obtain clear results, we adopt simplifying assumptions regarding the control process, i.e., we assume the control plant is an ideal integral chain with the known input gain coefficient, namely in Eq. (41) $a_i = 0$ and $\hat{b} = b$. To facilitate the computations, we replace Eqs. (52)-(55) by more general forms: $G_{\mathrm{PF}} = \nu\frac{\varphi_o(s)}{\varphi(s)}$ and $G_{\mathrm{FB}} = \frac{\mu(s)}{\varphi(s)}$, where $\nu \in \mathbb{R}$. For the process defined by $G_p(s) = bs^{-n}$, one can find $G_{\mathrm{CL}}(s) = \frac{Y(s)}{R(s)}$ as

$$G_{\mathrm{CL}}(s) = \nu\frac{\varphi_o(s)}{\varphi(s)}\frac{\varphi(s)}{s^n\varphi(s)+\mu(s)} = \frac{\nu\varphi_o(s)}{s^n\varphi(s)+\mu(s)} = \frac{\nu\varphi_o(s)}{\varphi_c(s)\varphi_o(s)}. \quad (63)$$

Recalling the particular parameterization for ADRC and IDRC given by Eqs. (12) and (21) and taking into account that $\nu = k_1 = \omega_c^n$ for ADRC and $\nu = \kappa_{\mathrm{int}} = \omega_c^{n+1}$ for IDRC, one can

Table 2. Comparison between $G_{\mathrm{PF}}(s)$ in both ADRC and IDRC approach for different order n of the algorithm; coefficients responded for system robustness are marked by red

n	ADRC	IDRC
1	$\frac{k_1\left(s^2+l_1 s+l_2\right)}{s^2+(k_1+l_1)s}$	$\frac{\kappa_{\mathrm{int}}(s+\iota_1)}{s^2+(\kappa_1+\iota_1)s}$
2	$\frac{k_1\left(s^3+l_1 s^2+l_2 s+l_3\right)}{s^3+(k_2+l_1)s^2+(k_1+l_2+k_2 l_1)s}$	$\frac{\kappa_{\mathrm{int}}\left(s^2+\iota_1 s+\iota_2\right)}{s^3+(\kappa_2+\iota_1)s^2+(\kappa_1+\iota_2+\kappa_2\iota_1)s}$
3	$\frac{k_1\left(s^4+l_1 s^3+l_2 s^2+l_3 s+l_4\right)}{s^4+(k_3+l_1)s^3+(k_2+l_2+k_3 l_1)s^2+(k_1+l_3+k_2 l_1+k_3 l_2)s}$	$\frac{\kappa_{\mathrm{int}}\left(s^3+\iota_1 s^2+\iota_2 s+\iota_3\right)}{s^4+(\kappa_3+\iota_1)s^3+(\kappa_2+\iota_2+\kappa_3\iota_1)s^2+(\kappa_1+\iota_3+\kappa_2\iota_1+\kappa_3\iota_2)s}$

Table 3. Comparison between $G_{\mathrm{FB}}(s)$ in both ADRC and IDRC approach for different order n of the algorithm; coefficients responded for system robustness are marked by red

n	ADRC	IDRC
1	$\frac{(l_2+k_1 l_1)s+k_1 l_2}{s^2+(k_1+l_1)s}$	$\frac{(\kappa_{\mathrm{int}}+\kappa_1\iota_1)s+\kappa_{\mathrm{int}}\iota_1}{s^2+(\kappa_1+\iota_1)s}$
2	$\frac{(l_3+k_1 l_1+k_2 l_2)s^2+(k_1 l_2+k_2 l_3)s+k_1 l_3}{s^3+(k_2+l_1)s^2+(k_1+l_2+k_2 l_1)s}$	$\frac{(\kappa_{\mathrm{int}}+\kappa_1\iota_1+\kappa_2\iota_2)s^2+(\kappa_1\iota_2+\kappa_{\mathrm{int}}\iota_1)s+\kappa_{\mathrm{int}}\iota_2}{s^3+(\kappa_2+\iota_1)s^2+(\kappa_1+\iota_2+\kappa_2\iota_1)s}$
3	$\frac{(l_4+k_1 l_1+k_2 l_2+k_3 l_3)s^3+(k_1 l_2+k_2 l_3+k_3 l_4)s^2+(k_1 l_3+k_2 l_4)s+k_1 l_4}{s^4+(k_3+l_1)s^3+(k_2+l_2+k_3 l_1)s^2+(k_1+l_3+k_2 l_1+k_3 l_2)s}$	$\frac{(\kappa_{\mathrm{int}}+\kappa_1\iota_1+\kappa_2\iota_2+\kappa_3\iota_3)s^3+(\kappa_1\iota_2+\kappa_2\iota_3+\kappa_{\mathrm{int}}\iota_1)s^2+(\kappa_1\iota_3+\kappa_{\mathrm{int}}\iota_2)s+\kappa_{\mathrm{int}}\iota_3}{s^4+(\kappa_3+\iota_1)s^3+(\kappa_2+\iota_2+\kappa_3\iota_1)s^2+(\kappa_1+\iota_3+\kappa_2\iota_1+\kappa_3\iota_2)s}$

find the following

$$G_{\mathrm{CL}}^{\mathrm{ADRC}}(s)=\frac{\omega_c^n\,(s+\omega_o)^{n+1}}{(s+\omega_o)^{n+1}\,(s+\omega_c)^n}, \tag{64}$$

and

$$G_{\mathrm{CL}}^{\mathrm{IDRC}}(s)=\frac{\omega_c^{n+1}\,(s+\omega_o)^n}{(s+\omega_o)^n\,(s+\omega_c)^{n+1}}, \tag{65}$$

where ω_c and ω_o are parameters that can be selected independently for both transfer functions, that is, one can choose different values of these parameters in (64) and (65).

Remark 5. *It is worth noting that the dynamics of the closed control loop in the IDRC approach is always characterized by an order one higher compared to the ADRC. This has consequences in the properties of both systems, for example, enforcing the same speed for n-th order system as in an $(n+1)$-th order system will imply differences in stability margins of the control loop.*

Attempting to match the dynamics Eq. (64) and Eq. (65), we assume that the nominal case is represented by Eq. (64) with fixed values of ω_o and ω_c. The task considered here is to find a tuning method for IDRC to obtain characteristics similar to those in the case of ADRC. For this purpose, we propose the following parametrizations of IDRC:

1. α-parameterization

$$G_{\mathrm{CL}}^{\mathrm{IDRC}}(s)=\frac{(\omega_c^{\alpha})^{n+1}\,(s+\omega_o^{\alpha})^n}{(s+\omega_o^{\alpha})^n\,(s+\omega_c^{\alpha})^{n+1}}, \tag{66}$$

with $\omega_o^{\alpha}=\alpha\omega_o$ and $\omega_c^{\alpha}=\alpha\omega_c$, which simply means that the observer and closed-loop bandwidth (from ADRC) in the IDRC approach are scaled by the $\alpha>0$ coefficient. Both bandwidths are scaled to maintain their ratio (modifying the relation between ω_o and ω_c will affect the stability of the closed-loop system). To obtain the algorithm gains, one can use the formula Eq. (24) assuming the observer and closed-loop system bandwidth values as ω_o^{α} and ω_c^{α}, respectively.

2. β-parameterization

$$G_{\mathrm{CL}}^{\mathrm{IDRC}}(s)=\frac{\beta\,\omega_c^{n+1}\,(s+\omega_o)^n}{(s+\omega_o)^n\,(s+\omega_c)^n\,(s+\beta\,\omega_c)}, \tag{67}$$

in which we are forcing the one pole of the closed-loop system to be non-dominant, by using the $\beta>1$ parameter. In general, increasing β implies that the $(n+1)$-th pole has a decreasing impact on the IDRC closed-loop dynamics.
Note that for the β-parameterization with $\beta\neq 1$, the controller gains cannot be selected using the formula from Eq. (24) due to the different desired poles of the closed-loop system. Instead, we want to obtain these gains satisfying the second condition from Eq. (20) with redefined desired polynomial of the closed-loop system

$$\det\left(s\mathbf{I}-\mathbf{H}_{\mathrm{CL}}^{\mathrm{IDRC}}\right)=(s+\beta\,\omega_c)(s+\omega_c)^n. \tag{68}$$

Consequently, the tuning rule for the controller introduced in Eq. (24) needs to be replaced by

$$\kappa_j=\begin{cases}\beta\,\omega_{\mathrm{c}}^{n+1} & \text{for } j=1,\\ \left[\beta\binom{n}{j-1}+\binom{n}{j-2}\right]\omega_{\mathrm{c}}^{n-j+2} & \text{for } j\in\{2,\ldots,n\},\end{cases} \tag{69}$$

with the integral gain $\kappa_{\mathrm{int}}=\kappa_1$.

Sensitivity analysis

This analysis is performed to present the relationship between signals from a closed-loop system (comparison of the sensitivity in different pathways) in the frequency domain. Such description is known as the "gang of six" presented in [24] and used with ADRC controller analysis in [25].

According to Fig. 3, the following control system model [25] can be investigated

$$\begin{bmatrix} Y(s) \\ U(s) \end{bmatrix} = \underbrace{\begin{bmatrix} G_{\mathrm{YR}} & G_{\mathrm{YD}} & G_{\mathrm{YD_M}} \\ G_{\mathrm{UR}} & G_{\mathrm{UD}} & G_{\mathrm{UD_M}} \end{bmatrix}}_{\mathbf{G}(s)} \begin{bmatrix} R(s) \\ D(s) \\ D_{\mathrm{M}}(s) \end{bmatrix}, \tag{70}$$

where relations from the transforms of signals: reference $R(s)$, external disturbance $D(s)$ and measurement noise $D_M(s)$, to the system output $Y(s)$ and control signal $U(s)$, are presented.

The transfer function matrix $\mathbf{G}(s)$ satisfies

$$\mathbf{G}(s) = \begin{bmatrix} \frac{\hat{b}^{-1}G_p(s)G_{\mathrm{PF}}(s)}{1+\hat{b}^{-1}G_p(s)G_{\mathrm{FB}}(s)} & \frac{G_p(s)}{1+\hat{b}^{-1}G_p(s)G_{\mathrm{FB}}(s)} & \frac{1}{1+\hat{b}^{-1}G_p(s)G_{\mathrm{FB}}(s)} \\ \frac{\hat{b}^{-1}(s)G_{\mathrm{PF}}(s)}{1+\hat{b}^{-1}G_p(s)G_{\mathrm{FB}}(s)} & \frac{-\hat{b}^{-1}G_{\mathrm{FB}}(s)G_{\mathrm{PF}}(s)}{1+\hat{b}^{-1}G_p(s)G_{\mathrm{FB}}(s)} & \frac{-\hat{b}^{-1}G_{\mathrm{FB}}(s)}{1+\hat{b}^{-1}G_p(s)G_{\mathrm{FB}}(s)} \end{bmatrix}, \tag{71}$$

where $G_p(s)$ is the transfer function of the control plant Eq. (4), containing its real parameters.

4. SIMULATION AND EXPERIMENTAL VALIDATION

This section presents the description of the control plant (mathematical model and system operation principles) and experimental results performed to confirm the theoretical considerations presented earlier. In particular, time responses for the proposed tuning methods and frequency characteristics of the control system components are presented.

4.1. Mathematical model of the experimental system

The experimental results have been carried out on the real control plant – the ball balancing table (BBT), where the control objective is to obtain the reference ball position on the plate (Fig. 4a). The measurement signal is read by a touch-resisting panel. The control signal is considered as the desired rotation of the servomotor arm. The internal control loop is realized in hardware, and then there is the dynamics between servomotor rotation and ball position. Exemplary equations of movement for the considered system can be found in [26], whereas application using ADRC in [27]. Assuming the movement in two axes (x and y positions), the nonlinear BBT model is given by

$$\begin{cases} \ddot{x} = -\frac{mr_b^2}{mr_b^2+J}\left(\dot{\theta}_x\dot{\theta}_y y + \dot{\theta}_x^2 x - g\sin\theta_x\right), \\ \ddot{y} = -\frac{mr_b^2}{mr_b^2+J}\left(\dot{\theta}_x\dot{\theta}_y x + \dot{\theta}_y^2 y - g\sin\theta_y\right), \end{cases} \tag{72}$$

where $\theta_{x/y}$ is the angle of the platform (input signal), x and y are the ball position coordinates (output signals), m is the ball mass, J is the moment of inertia of the ball, r_b is the ball radius, g is the gravitational acceleration.

The mentioned model (after linearization) presents the second-order integrator, assumed as the nominal plant for ADRC and IDRC control. Note that Eq. (72) does not show the whole plant model. The differential equations after including the actuator dynamics are derived below.

In this work, one degree of freedom – y axis – is considered (Fig. 4b) to show the proposed tuning rules without introducing additional disturbances from cross-coupling. Therefore, the y signal is the system output, and the input signal u is the desired servo rotation angle for the y axis. One can assume that the internal control loop of the servomotor arm position is approximated by the first-order inertia system

$$\dot{\upsilon} = -\tau^{-1}\upsilon + \tau^{-1}u, \tag{73}$$

where υ and u are the actual and desired motor arm angles, τ is the control loop time constant.

The dependency between the plate and servo angles is

$$\theta_y = r_m L^{-1}\upsilon, \tag{74}$$

where r_m is the motor arm length and L is the plate length in the y axis.

After combining Eq. (74), Eq. (73) and the second equation from Eq. (72), and under the assumption of small angles values $u \to 0$, a simplified linear model for the considered control object is described by a third-order differential equation with a structure corresponding to Eq. (1)

$$y^{(3)} = bu\overbrace{-a_2\ddot{y} + d + g(\cdot)}^{f(\cdot)}, \tag{75}$$

where y is the measured output (ball position) u is the desired servomotor angle (input signal), d is the disturbance signal (additional displacement of the servo), $g(\cdot)$ is the unmodeled dynamics part and linearization errors relative to structure Eq. (75). The real values of plant parameters are $a_2 = \frac{1}{\tau} = 66.67$ and $b = \frac{mgr_b^2 r_m}{\tau(mr_b^2+J)L} = 114.6$.

The transfer function representation of the system Eq. (72) linear part (where $d = 0$ and $g(\cdot) = 0$) is expressed as

$$G_p(s) = \frac{b}{s^3 + a_2 s^2}, \tag{76}$$

and is introduced for theoretical considerations, to be used for closed-loop system model calculations in the following sections (parameter a_2 was not used in the control synthesis).

The derivation of the third-order BBT model is presented in [28]. Generally, the model is nonlinear with strong cross-coupling disturbances. The linear approximation of this model represents the second-order integrator connected to an inertial system with a small time constant. The influence of plant parameters on the ADRC operation quality and stability has been presented in more detail in [29].

The physical constraints of the system are given as follows

$$\begin{cases} 0.00\,\mathrm{m} \le y \le 0.30\,\mathrm{m}, \\ -0.785\,\mathrm{rad} \le u \le 0.785\,\mathrm{rad}. \end{cases} \tag{77}$$

In addition, it is noteworthy that the same experimental setup was also used in [30, 31]. However, these papers address different problems, focusing on the ADRC methodology for state and disturbance estimation in the presence of measurement noise as well as the issue of input gain parameter

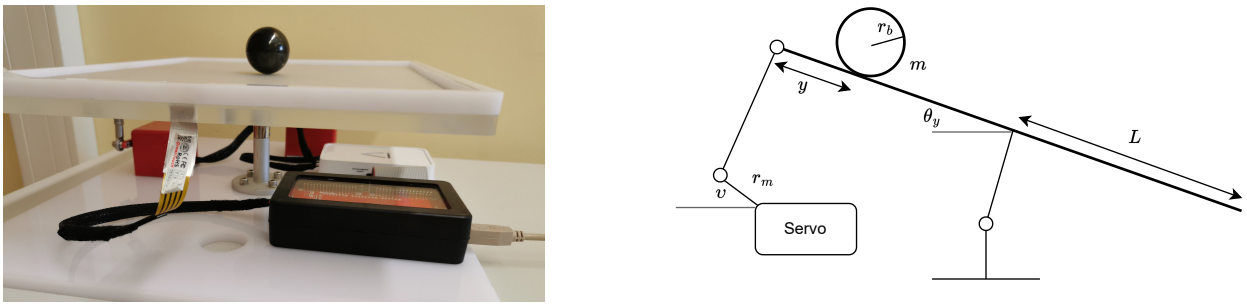

(a) Photo of the used control plant **(b)** Diagram of simplified system operation

Fig. 4. The considered BBT system with its laboratory testbed (left) and schematic diagram for the y axis (right)

selection and order reduction of the model in the ADRC algorithm, respectively. In the current work, the setup is used to conduct experiments that verify the theoretical comparison and tuning methods proposed for the ADRC and IDRC structures.

4.2. Comparison of both methods using proposed parameterizations for IDRC

Sensitivity analysis

The magnitude Bode plots are presented for the "gang of six" considered in Eq. (71) using the BBT model Eq. (76) as the plant transfer function. The simulation results for α- and β-parameterization can be found in Figs. 5 and 6.

Based on the results, it can be concluded that for both α- and β-parameterizations in the IDRC approach, the character of relations between signals in a closed-loop system is similar to ADRC. The main difference between ADRC and IDRC approaches can be observed in relative order of G_{YR}, G_{UR} and G_{UD} transfer functions, whose numerator includes the prefilter transfer function Eq. (71). The relative order of G_{PF} is different in both approaches due to the extension of the state in ADRC.

In general, a slight change in the α parameter implies greater changes in closed-loop sensitivity, because we are scaling both the observer and the controller bandwidth. Using β-parameterization, we only force the $(n+1)$-th pole to be non-dominant, leading to less pronounced changes in characteristics, which are more noticeable at higher frequencies.

According to detailed relationships in the closed-loop system for the assumed case, the external disturbance-to-output (G_{YD}) transfer function characteristics show that the IDRC tuned using α-parameterizations can offer both better and worse attenuation of constant disturbances $(\Omega \to 0)$ than the ADRC approach, depending on the value α. From Fig. 5 it can be seen that $\alpha = 1.45$ corresponds to the same attenuation of constant disturbances in both ADRC and IDRC approaches. In β-parameterization it can be concluded that for $\beta > 5$ the characteristics of the G_{YD}) transfer function are similar in both approaches. The attenuation of high-frequency disturbances (e.g., unmodeled part of system dynamics) is equal for both approaches with any parameterization of IDRC.

The $G_{\mathrm{YD_M}}$ and $G_{\mathrm{UD_M}}$ represent the sensitivity of the output and control signal sensitivity to measurement noise, whose magnitude plots are similar (taking into account the whole bandwidth) for any IDRC parameterization, so the differences within the changes α or β are almost unnoticeable in closed-loop system performance.

Results from experiments

The considered control objective is to bring the ball to the reference position in the middle of the table $r = 0.15$ m, starting from the edge of the table for $y(0) = 0$ m. The control algorithm gains (for both ADRC and IDRC) $\hat{b} = 28.65$, $\omega_c = 2.8$, $\omega_o = 28$ were assumed. The system order for experimental purposes was assumed as a real one $n = 3$. To check the robustness of the external disturbance, an additional signal was introduced in the input path $d(t) = 0.26 \cdot \mathbf{1}(t-20)$ rad. This means forcing the servo motor arm to move 15 degrees halfway through the experiment time. The experimental results using α- and β-parameterization are shown in Figs. 7a and 7b. The numerical values of the observer and state feedback gains for the considered experiment scenarios can be found in Tab. 4.

Based on the experimental results, it can be observed that the proposed IDRC parameterizations ensure closed-loop system performance consistent with theoretical considerations. For higher values of the α parameter, a less aggressive response of the closed-loop system is observed to the reference and disturbance signals. Specifically, for $\alpha = 1.5$, the disturbance responses for both the ADRC and IDRC approaches are very similar. This is consistent with the theoretical considerations for $\alpha = 1.45$, as shown in the Bode plots.

In the case of β-parameterization, the response character within the considered gain range is more similar to each other compared to the previous case. This is confirmed by the relatively small scope of the changes in the modulus plots. In terms of measurement noise dependency, the same frequency components of the control signal for both parameterizations are visible. These results confirm the relationships presented by the "gang of six".

5. CONCLUSIONS

In this work, we have shown that an approach combining a standard, textbook state-feedback control with an integral compensator (denoted here as IDRC) can be derived in the form of an active disturbance rejection scheme. This means that the observer part no longer has to be equipped with a plant model

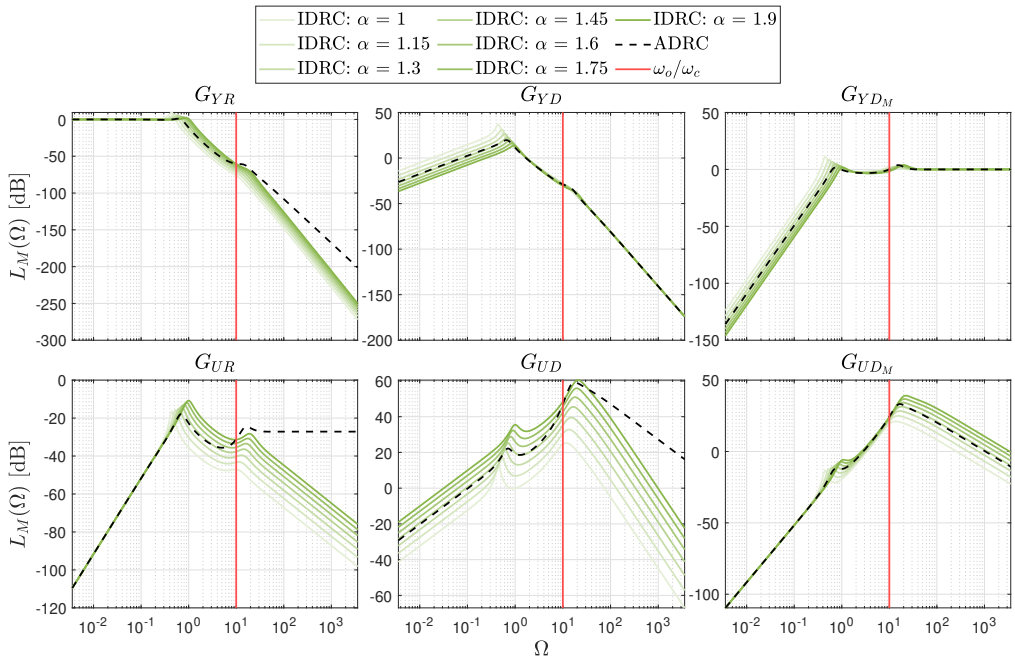

Fig. 5. Results from the simulation – magnitude characteristics for "gang of six" components assuming BBT model for different α values where $n = 3$, $\omega_o = 28$, $\omega_c = 2.8$, $\hat{b} = 28.65$. Characteristics collected for normalized frequency $\Omega = \omega/\omega_c$. The ω_o/ω_c ratio is marked by a red line.

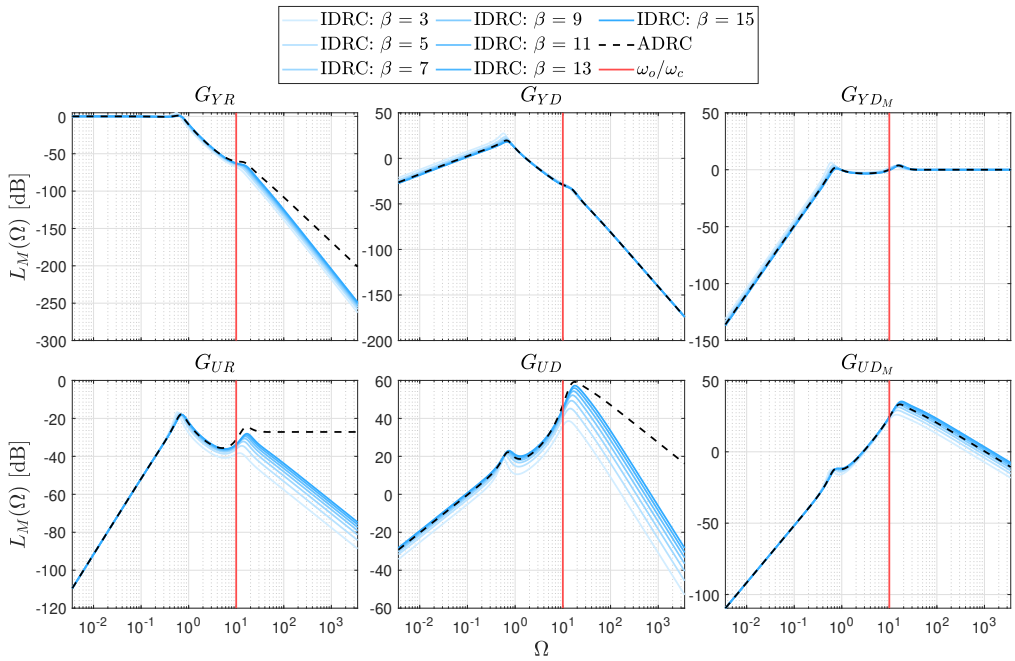

Fig. 6. Results from the simulation – magnitude characteristics for "gang of six" components assuming BBT model for different β values where $n = 3$, $\omega_o = 28$, $\omega_c = 2.8$, $\hat{b} = 28.65$. Characteristics collected for normalized frequency $\Omega = \omega/\omega_c$. The ω_o/ω_c ratio is marked by a red line.

as accurately as possible since for ADRC-like schemes, one deliberately makes the (erroneous) assumption of an integrator chain model, regardless of the actual plant behavior. Such a methodology greatly simplifies plant modeling and represents a departure from the established school of control based on accurate plant modeling. In other words, it was shown that the disturbance-centric methodology of ADRC can work like an enabler that can lead to the robustification of classic controllers. The found equivalence also means that a linear ADRC can be traced back to a "classical" observer-based state-feedback control with disturbance compensation and that an equivalence can be established (assuming certain parameterization). The significance behind being structurally equivalent to a well-known approach from linear control systems theory means that typical methods to analyze stability and performance criteria can, fortunately, be applied to ADRC as well,

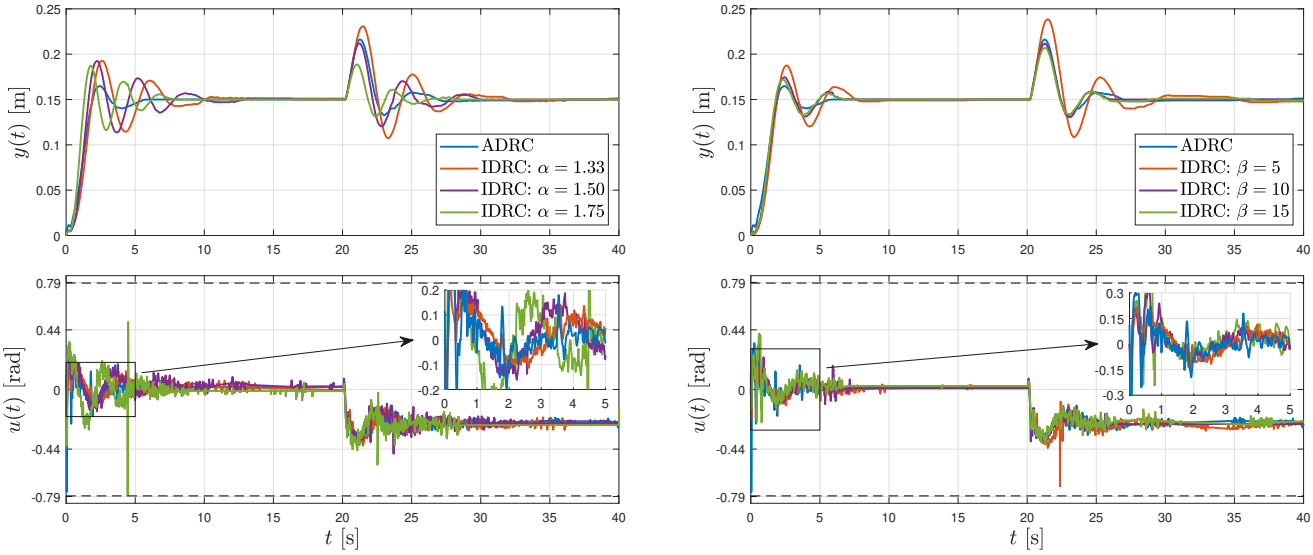

(a) Result from experiments for α-parameterization

(b) Result from experiments for β-parameterization

Fig. 7. Results from the experiments on BBT system for different α and β values in IDRC approach where $n = 3$, $\omega_o = 28$, $\omega_c = 2.8$, $\hat{b} = 28.65$. System output and control signal. Control signal limits are marked by the dashed lines.

Table 4. Observer and controller gains values for the parameterizations used in the experiments.

Gains		ADRC	Gains	IDRC					
		$\omega_o = 28$, $\omega_c = 2.8$		α			β		
				1.33	1.50	1.75	5	10	15
Observer	l_1	112	ι_1	112	126	147	84	84	84
	l_2	4704	ι_2	4160	5292	7203	2352	2352	2352
	l_3	87808	ι_3	51645	74088	117649	21952	21952	21952
	l_4	614656	ι_4	—	—	—	—	—	—
Controller	k_1	22.95	κ_1	206.58	293.35	470.60	351.23	680.51	1009.80
	k_2	23.52	κ_2	83.21	105.84	144.06	141.12	258.72	376.32
	k_3	8.40	κ_3	14.90	16.80	19.60	22.40	36.40	50.40
	k_4	—	κ_{int}	192.32	311.17	576.48	307.33	614.66	921.98

thus showing its backward compatibility.

As for future work, there is a need to study the influence of design parameters on the control system performance for ADRC and IDRC approaches. Various plant types can be used, including the BBT. How this affects the claims made in this work remains an open point.

REFERENCES

[1] E. Sariyildiz, R. Oboe, and K. Ohnishi, "Disturbance observer-based robust control and its applications: 35th anniversary overview," *IEEE Transactions on Industrial Electronics*, vol. 67, no. 3, pp. 2042–2053, 2020.

[2] X. Zhang, X. Zhang, W. Xue, and B. Xin, "An overview on recent progress of extended state observers for uncertain systems: methods, theory, and applications," *Advanced Control for Applications*, vol. 3, no. 2, 2021.

[3] J. Han, "From PID to active disturbance rejection control," *IEEE Transactions on Industrial Electronics*, vol. 56, no. 3, pp. 900–906, 2009.

[4] Z. Gao, "Active disturbance rejection control: From an enduring idea to an emerging technology," in *International Workshop on Robot Motion and Control*, 2015, pp. 269–282.

[5] M. Stankovic, H. Ting, and R. Madonski, "From PID to ADRC and back: Expressing error-based active disturbance rejection control schemes as standard industrial 1DOF and 2DOF controllers," *Asian Journal of Control*, 2024.

[6] M. Huba and Z. Gao, "Uncovering disturbance observer and ultra-local plant models in series PI controllers," *Symmetry*, vol. 14, no. 4, 2022.

[7] R. Madonski, G. Herbst, and M. Stankovic, "ADRC in output and error form: connection, equivalence, performance," *Control Theory and Technology*, vol. 21, pp. 56–71, 2023.

[8] G. Herbst and R. Madonski, "Tuning and implementation variants of discrete-time ADRC," *Control Theory and Technology*, vol. 21, no. 1, pp. 72–88, 2023.

[9] M. Huba, "Disturbance observer in PID controllers for

first-order time-delayed systems," *IFAC-PapersOnLine*, vol. 55, no. 17, pp. 19–24, 2022.

[10] S. Zhong, Y. Huang, and L. Guo, "A parameter formula connecting PID and ADRC," *Science China Information Sciences*, vol. 63, no. 9, 2020.

[11] Z. Gao, "Scaling and bandwidth-parameterization based controller tuning," in *American Control Conference*, 2003, pp. 4989–4996.

[12] Z. Wu, Makeximu, J. Yuan, Y. Liu, D. Li, and Y. Chen, "A synthesis method for first-order active disturbance rejection controllers: procedures and field tests," *Control Engineering Practice*, vol. 127, 2022.

[13] S. Zhong, Y. Huang, and L. Guo, "An ADRC-based PID tuning rule," *International Journal of Robust and Nonlinear Control*, pp. 1–14, 2022.

[14] H. Sira-Ramirez, E. W. Zurita-Bustamante, and C. Huang, "Equivalence among flat filters, dirty derivative-based PID controllers, ADRC, and integral reconstructor-based sliding mode control," *IEEE Transactions on Control Systems Technology*, vol. 28, no. 5, pp. 1696–1710, 2020.

[15] H. Sira-Ramirez and E. Zurita-Bustamante, "On the equivalence between ADRC and flat filter based controllers: a frequency domain approach," *Control Engineering Practice*, vol. 107, p. 104656, 2021.

[16] S. Ahmad and A. Ali, "Unified disturbance-estimation-based control and equivalence with IMC and PID: case study on a DC–DC boost converter," *IEEE Transactions on Industrial Electronics*, vol. 68, no. 6, pp. 5122–5132, 2021.

[17] R. Chi, H. Zhang, H. Li, B. Huang, and Z. Hou, "Data-driven dynamic internal model control," *IEEE Transactions on Cybernetics*, pp. 1–13, 2024.

[18] Z. Gao and Y. Huang, "Connecting theory and practice with ADRC," *Control Theory and Technology*, vol. 21, no. 1, pp. 1–3, 2023.

[19] K. Aida and T. Kitamori, "Design of a PI-type state feedback optimal servo system," *International Journal of Control*, vol. 52, no. 3, pp. 613–625, 1990.

[20] Y. Zhao, Y. Huang, and Z. Gao, "On tuning of ADRC with competing design indices: a quantitative study," *Control Theory and Technology*, vol. 21, no. 1, pp. 16–33, 2023.

[21] J. A. Gouvêa, L. M. Fernandes, M. F. Pinto, and A. R. Zachi, "Variant adrc design paradigm for controlling uncertain dynamical systems," *European Journal of Control*, vol. 72, p. 100822, 2023.

[22] R. Patelski and D. Pazderski, "Improving the active disturbance rejection controller tracking quality by the input-gain underestimation for a second-order plant," *Electronics*, vol. 10, no. 8, p. 907, 2021.

[23] H. Jin and Z. Gao, "On the notions of normality, locality, and operational stability in ADRC," *Control Theory and Technology*, vol. 21, no. 1, pp. 97–109, 2023.

[24] K. J. Åström and R. Murray, *Feedback systems: An introduction for scientists and engineers*. Princeton University Press, 2008.

[25] G. Herbst, "Transfer function analysis and implementation of active disturbance rejection control," *Control Theory and Technology*, vol. 19, pp. 19–34, 2021.

[26] M. Hamdoun, M. B. Abdallah, M. Ayadi, F. Rotella, and I. Zambettakis, "Functional observer-based feedback controller for ball balancing table," *SN Applied Sciences*, vol. 3, no. 614, 2021.

[27] Z. Wu, G. Shi, D. Li, Y. Liu, and Y. Chen, "Active disturbance rejection control design for high-order integral systems," *ISA Transactions*, vol. 125, pp. 560–570, 2022.

[28] M. Mrotek and J. Michalski, "Trajectory tracking with generalized active disturbance rejection control using kalman filter-based extended state observer," in *International Conference on Methods and Models in Automation and Robotics*. IEEE, 2024, pp. 316–321.

[29] J. Michalski, M. Mrotek, M. Retinger, and P. Kozierski, "Adaptive active disturbance rejection control with recursive parameter identification," *Electronics*, vol. 13, no. 16, p. art. no. 3114, 2024.

[30] J. Michalski, M. Mrotek, and P. Kozierski, "Kalman filter as an alternative to extended state observer in ADRC control algorithm," *Pomiary Automatyka Robotyka*, vol. 28, no. 1, pp. 31–39, 2024, (in Polish).

[31] J. Michalski, M. Mrotek, and S. Brock, "Transfer function analysis and algorithm order reduction for active disturbance rejection control," in *International Conference on Methods and Models in Automation and Robotics*. IEEE, 2024, pp. 591–596.